

# Diffuse right ventricular fibrosis in heart failure with preserved ejection fraction and pulmonary hypertension

Ravi B. Patel<sup>1</sup>, Emily Li<sup>1</sup>, Brandon C. Benefield<sup>2</sup>, Stanley A. Swat<sup>1</sup>, Vincenzo B. Polsinelli<sup>1</sup>, James C. Carr<sup>3</sup>, Sanjiv J. Shah<sup>1</sup>, Michael Markl<sup>3,4</sup>, Jeremy D. Collins<sup>5</sup> and Benjamin H. Freed<sup>1\*</sup>

<sup>1</sup>Division of Cardiology, Northwestern University, Chicago, IL, USA; <sup>2</sup>Feinberg Cardiovascular and Renal Research Institute, Northwestern University, Chicago, IL, USA; <sup>3</sup>Department of Radiology, Northwestern University, Chicago, IL, USA; <sup>4</sup>Department of Biomedical Engineering, Northwestern University, Chicago, IL, USA; <sup>5</sup>Department of Radiology, Mayo Clinic, Rochester, MN, USA

## Abstract

**Aims** While right ventricular (RV) dysfunction is associated with worse prognosis in co-morbid pulmonary hypertension and heart failure with preserved ejection fraction (PH-HFpEF), the mechanisms driving RV dysfunction are unclear. We evaluated the extent and clinical correlates of diffuse RV myocardial fibrosis in PH-HFpEF, as measured by cardiovascular magnetic resonance-derived extracellular volume (ECV).

**Methods and results** We prospectively enrolled participants with PH-HFpEF ( $n = 14$ ), pulmonary arterial hypertension (PAH;  $n = 13$ ), and controls ( $n = 8$ ). All participants underwent high-resolution cardiovascular magnetic resonance, and case subjects (PH-HFpEF and PAH) additionally underwent right heart catheterization. T1 mapping was performed using high-resolution modified look-locker inversion recovery with a  $1 \times 1 \text{ mm}^2$  in-plane resolution. RV free wall T1 values were quantified, and ECV was calculated. Participants with PH-HFpEF were older and carried higher rates of hypertension and obstructive sleep apnoea than those with PAH. While RV ECV was similar between PH-HFpEF and PAH ( $33.1 \pm 8.0$  vs.  $34.0 \pm 4.5\%$ ;  $P = 0.57$ ), total pulmonary resistance was lower in PH-HFpEF compared with PAH [PH-HFpEF:  $5.68 \text{ WU}$  ( $4.70, 7.66 \text{ WU}$ ) vs. PAH:  $8.59 \text{ WU}$  ( $8.14, 12.57 \text{ WU}$ );  $P = 0.01$ ]. RV ECV in PH-HFpEF was associated with worse indices of RV structure (RV end-diastolic volume:  $r = 0.67$ ,  $P = 0.01$ ) and RV function (RV free wall strain:  $r = 0.59$ ,  $P = 0.03$ ) but was not associated with RV afterload (total pulmonary resistance:  $r = 0.08$ ,  $P = 0.79$ ). Conversely, there was a strong correlation between RV ECV and RV afterload in PAH ( $r = 0.57$ ,  $P = 0.04$ ).

**Conclusions** Diffuse RV fibrosis, as measured by ECV, is present in PH-HFpEF and is associated with adverse RV structural and functional remodelling but not degree of pulmonary vasculopathy. In PH-HFpEF, diffuse RV fibrosis may occur out of proportion to the degree of RV afterload.

**Keywords** Heart failure with preserved ejection fraction; Right ventricle; Fibrosis; Pulmonary hypertension; Cardiac magnetic resonance

Received: 8 August 2019; Revised: 4 October 2019; Accepted: 4 November 2019

\*Correspondence to: Benjamin H. Freed, Division of Cardiology, Department of Medicine, Northwestern University Feinberg School of Medicine, 676 N St Clair St., Suite 600, Chicago, IL 60611, USA. Tel: 312-926-8948; Fax: 312-926-8250.

Email: benjamin.freed@northwestern.edu

## Introduction

Right ventricular (RV) dysfunction is a common pathophysiological consequence of heart failure with preserved function (HFpEF), and its presence predicts a worse prognosis.<sup>1–5</sup> RV

dysfunction is linked to co-morbid pulmonary hypertension (PH-HFpEF) and is associated with a 1 year mortality of  $>25\%$ .<sup>6,7</sup> Despite the prognostic significance of RV dysfunction in HFpEF, little is known about its underlying mechanisms in this patient population. While RV dysfunction in PH-HFpEF

may be driven by either increased RV afterload [due to elevated left ventricular (LV) filling pressures] or load-independent mechanisms, the relative contributions of these processes remain unclear. The degree of diffuse RV fibrosis in PH-HFpEF, as measured by cardiovascular magnetic resonance (CMR) imaging-derived extracellular volume (ECV), has not been described and may provide further insight into pathophysiological mechanisms driving RV dysfunction and poor outcomes in this cohort.

Attempts to quantify RV ECV have been challenging because of spatial resolution limitations imaging the thin-walled RV myocardium. Using high-resolution CMR T1 mapping specifically designed to evaluate ECV expansion of the RV, we sought to better characterize the RV myocardial structural changes associated with PH-HFpEF. We aimed to (i) determine the presence and degree of RV fibrosis in patients with PH-HFpEF, (ii) explore the relationships between RV fibrosis and indices of RV structure and function, and (iii) identify differences in haemodynamic and imaging parameters associated with diffuse RV fibrosis between PH-HFpEF and pulmonary arterial hypertension (PAH). We hypothesized that patients with PH-HFpEF have a significantly higher amount of RV fibrosis compared with controls and have similar or greater RV fibrosis than PAH patients despite lower RV afterload.

## Methods

### Study population

Between March 2014 and December 2016, case subjects with PH-HFpEF or PAH were prospectively enrolled after undergoing a clinically indicated right heart catheterization at Northwestern Memorial Hospital. Inclusion criteria for PH-HFpEF were mean pulmonary artery pressure  $\geq 25$  mmHg at rest, pulmonary capillary wedge pressure  $\geq 15$  mmHg, LV ejection fraction (LVEF)  $\geq 55\%$ , and signs/symptoms of heart failure as defined by Framingham criteria in the last 12 months.<sup>8</sup> Inclusion criteria for PAH were mean pulmonary arterial pressure of  $\geq 25$  mmHg at rest, and pulmonary capillary wedge pressure was  $< 15$  mmHg. Age-matched and gender-matched subjects with no known cardiovascular disease were included as controls.

Exclusion criteria included the presence of greater than moderate valvular disease, World Health Organization Group III–V PH, previous cardiac or pulmonary transplantation, previous history of reduced LVEF  $< 40\%$  (i.e. recovered LVEF), implantable cardioverter defibrillator or pacemaker implantation, claustrophobia, other contraindications to MRI, or a glomerular filtration rate  $< 30$  mL/min/1.73 m<sup>2</sup>. All study participants gave written informed consent, and the institutional review board at Northwestern University approved the study.

### Clinical characteristics

We collected the following data in all study participants: demographics, New York Heart Association (NYHA) functional class, co-morbidities, medications, vital signs, body mass index, and laboratory data, including creatinine and haematocrit. Co-morbidity definitions are listed in Supporting Information, *Data S1*.

### Cardiovascular magnetic resonance protocol

All case subjects and controls underwent comprehensive CMR at 1.5T (MAGNETOM Aera, Siemens Healthineers, Erlangen, Germany). Haematocrit and creatinine were drawn in each subject prior to starting the scan. Blood pressure and heart rate were recorded prior to and after CMR acquisition. The imaging protocol consisted of balanced steady-state free precession cine imaging, high-resolution pre-contrast and post-contrast T1 mapping, and late gadolinium enhancement (LGE) imaging. The total scan time was approximately 70 min.

### Cardiovascular magnetic resonance fibrosis assessment

Pre-contrast T1 mapping was performed in an oblique axial orientation orthogonal to the RV free wall using a 5(3)3 modified look-locker imaging (MOLLI) sequence utilizing an 11-heartbeat acquisition comprising two look-locker cycles (five-heartbeat and three-heartbeat duration, respectively), separated by a recovery period of three heartbeats. The two look-locker cycles were used to sample T1 recovery with single-shot balanced steady-state free precession diastolic readouts. A three-heartbeat pause was inserted between look-locker cycles to allow recovery of longitudinal magnetization. Post-contrast T1 mapping was performed with identical slice positioning utilizing a 4(1)3(1)2 MOLLI sequence, composed of three look-locker cycles separated by recovery periods of one-heartbeat duration. The distinct pre-contrast and post-contrast T1 look-locker experiments enable optimal sampling of the T1 recovery curve for the expected myocardial and blood pool values in the presence and absence of gadolinium-based contrast media, respectively.

The high-resolution MOLLI (HR-MOLLI) sequence was acquired with an in-plane spatial resolution of  $1 \times 1$  mm<sup>2</sup>. Typical pulse sequence parameters included: flip angle =  $35^\circ$ , field of view =  $280 \times 210$  mm<sup>2</sup>,  $272 \times 174$  matrix, gradient recalled autocalibrating partial parallel acquisition factor 2, 6/8ths partial Fourier, and slice thickness = 8 mm. HR-MOLLI sequences were acquired with breath holding at end expiration, with a 5 s pause from the initiation of the breath hold to the start of the scan. Shot time for the 5(3)3 and 4(1)3(1)2 HR-MOLLI iterations was 228 m.

Data were processed in-line using a motion-correction algorithm with automated T1 parametric map generation.<sup>9</sup> Images with significant motion degradation were reviewed at the scanner and repeated as needed. Images were acquired before and between 10 and 25 min after 0.2 mmol/kg gadopentetate dimeglumine (Magnevist, Bayer Healthcare, Whippany, NJ) infusion. Pre-contrast and post-contrast HR-MOLLI acquisitions were obtained in each subject (*Figure 1*).

### Cardiovascular magnetic resonance analysis

Regions of interest were drawn on pre-contrast and post-contrast HR-MOLLI images using QMass MR 7.6 (Medis, Leiden, The Netherlands) (*Figure 1*). RV native T1 values were determined on pre-contrast T1 parametric maps from the free wall in the basal and mid-chamber and averaged together. LV native T1 values were determined on pre-contrast T1 parametric maps from the lateral wall. Post-contrast T1 values were obtained from matching locations on post-contrast HR-MOLLI parametric maps. Cine images were used to confirm absence of fatty metaplasia. Focal areas of fibrosis were avoided. LV blood pool T1 values were obtained from corresponding parametric maps taking care to exclude chamber trabeculae by review of the non-motion-corrected MOLLI images. ECV values were calculated using the published formula<sup>10</sup>:

$$ECV = (1 - \text{haematocrit}) * [\Delta R1_{\text{myocardium}}] / [\Delta R1_{\text{blood pool}}],$$

where  $\Delta R1 = R1^{\text{post-contrast}} - R1^{\text{pre-contrast}}$  and  $R1 = 1/T1$ . Two experienced CMR readers analysed all HR-MOLLI data.

Intra-observer variability of RV native T1 and RV ECV was assessed in 12 subjects by having the same observer repeat the analysis at least 6 months apart. A second independent observer repeated the analysis of all 12 subjects to assess inter-observer variability for RV native T1 and RV ECV.

Details for analysis of biventricular systolic function, RV longitudinal strain, and LGE are included in Supporting Information, *Data S1*.

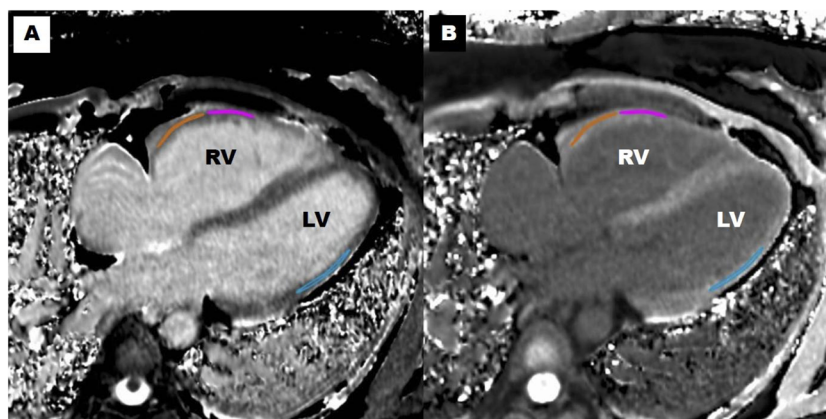
### Comprehensive echocardiography and invasive haemodynamics

Echocardiography was performed in a subset of the case subjects using a systematic protocol as detailed in Supporting Information, *Data S1*. Right-sided heart catheterization was performed in PH-HFpEF and PAH as described in Supporting Information, *Data S1*.

### Statistical analysis

Categorical variables were expressed as count and percentages and continuous variables with a normal distribution as mean  $\pm$  standard deviation. Non-normally distributed continuous variables were reported as median (25th percentile, 75th percentile). We used Student's *t*-test to compare the means of normally distributed continuous variables in PH-HFpEF and PAH subjects or the nonparametric Mann-Whitney *U* test as appropriate. Categorical variables were compared using Fisher's exact or  $\chi^2$  test. We compared RV ECV by NYHA class among case subjects using the one-way analysis of variance test. We examined the correlation between RV ECV with variables from echocardiography, invasive haemodynamics, and CMR using Pearson pairwise correlation. We evaluated the association between RV ECV and RV function as measured by RV free wall strain (dependent variable) using multivariable linear regression. Linear regression models were adjusted for total pulmonary resistance (TPR). Reproducibility data were reported using the intra-class correlation coefficient (ICC) and

**Figure 1** (A) Pre-contrast and (B) post-contrast T1 parametric maps using high-resolution modified look-locker inversion recovery image in a pulmonary hypertension subject. Orange and pink lines represent regions of interest in the right ventricular (RV) free wall. Blue line represents region of interest in the left ventricular (LV) lateral wall.



coefficient of variation (COV). Two-sided  $P$ -values  $<0.05$  were considered significant. All analyses were performed using STATA (Version 12, StataCorp, College Station, TX).

## Results

During the study period, 32 case subjects with PH-HFpEF or PAH underwent CMR testing after meeting the inclusion criteria. Two case subjects were excluded from final analysis because of poor image quality, two were excluded because of claustrophobia, and one was excluded because of LVEF  $<55\%$ . Therefore, 27 case subjects and eight controls were included for final analysis. Of the 27 case subjects, 14 met haemodynamic criteria for PH-HFpEF, and the remaining 13 subjects met haemodynamic criteria for PAH. Of the 13 subjects with PAH, all had World Health Organization Group I PAH (six had collagen vascular disease and seven had idiopathic PAH).

Compared with subjects with PAH, PH-HFpEF subjects were older with a higher frequency of systemic hypertension, hyperlipidaemia, and obstructive sleep apnoea (Table 1). A greater percentage of PH-HFpEF subjects were taking loop diuretics while significantly more PAH subjects were taking phosphodiesterase-5 inhibitors. On haemodynamic assessment, PH-HFpEF subjects had significantly lower pulmonary arterial pressure, lower transpulmonary gradient, higher pulmonary capillary wedge pressure, and lower TPR compared with PAH patients (Table 2).

### Imaging characteristics of pulmonary hypertension and heart failure with preserved ejection fraction, pulmonary arterial hypertension, and controls

Cardiovascular magnetic resonance was performed within  $25 \pm 12$  days of right heart catheterization. Biventricular size and function were not assessed in one subject with PH-HFpEF and one subject with PAH because of extensive gating artefact on cine images. Table 3 details the differences in CMR parameters between PH-HFpEF, PAH, and controls. Both PAH subjects and PH-HFpEF subjects had mildly reduced RV ejection fraction (RVEF) compared with controls. The presence of LGE was higher in PAH vs. PH-HFpEF. The majority of LGE (67%) was present in both the anterior and inferior RV insertion points. Participants with either PH-HFpEF or PAH had a higher degree of RV diffuse fibrosis compared with controls as measured by RV native T1 and RV ECV (Figure 2). There was no significant difference in LV native T1 or LV ECV between PH-HFpEF or PAH and controls.

Echocardiograms performed for clinical reasons [available in a subset of the case subjects ( $n = 24$ )] were analysed.

Two subjects with PAH were excluded because they had echocardiograms that were greater than 6 months prior to or after the time of their CMR. One PH-HFpEF subject was excluded because of extremely technically poor acoustic windows. Results are listed in Supporting Information, Table S1.

### Correlates of right ventricular extracellular volume in full cohort

When all case subjects (PH-HFpEF or PAH) and controls were combined, RV ECV had the strongest correlation with left atrial volume index, E/A ratio, and LV ECV (Supporting Information, Table S2). RV ECV did not significantly correlate with RVEF, and 36% of all subjects with normal RVEF had an elevated RV ECV (Figure 3). There was no significant difference in RV ECV by NYHA class (Class I:  $0.36 \pm 0.01$ , Class II:  $0.33 \pm 0.08$ , and Class III:  $0.38 \pm 0.06$ ,  $P = 0.21$ ). Correlates of LV ECV among all case subjects and among PH-HFpEF and PAH separately are detailed in Supporting Information, Tables S3 and S4, respectively.

### Clinical and imaging correlates of right ventricular extracellular volume in pulmonary hypertension and heart failure with preserved ejection fraction compared with pulmonary arterial hypertension

In PH-HFpEF, RV ECV strongly correlated with echocardiography-derived LVEF, echocardiography-derived left atrial volume index, RV diastolic stiffness, CMR-derived LV EDV index, CMR-derived RV EDV index, and RV free wall longitudinal strain (Table 4). In PAH, RV ECV strongly correlated with E/A ratio, PVR, and TPR from invasive haemodynamics (Table 4 and Figure 4).

### Association of right ventricular extracellular volume and right ventricular strain

In PH-HFpEF, higher RV ECV was independently associated with worse RV free wall strain after adjustment for TPR ( $\beta$  coefficient: 34.7, 95% confidence interval: 4.8, 64.5,  $P = 0.03$ ). There was no significant association between RV ECV and RV free wall strain after adjustment for TPR in the PAH cohort ( $\beta$  coefficient:  $-15.0$ , 95% confidence interval:  $-86.6$ , 56.5,  $P = 0.65$ ).

### Reproducibility of right ventricular native (pre-contrast) T1 and right ventricular extracellular volume

For intra-observer variability, we found that the ICC for RV native T1 was 0.80 and COV was 5.8%. The ICC for RV ECV was 0.91, and COV was 8.8%. For inter-observer variability,

**Table 1** Clinical characteristics of study cohort

Clinical characteristics	PAH (n = 13)	PH-HFpEF (n = 14)	P-value*	Control (n = 8)	P-value†
Age (years)	60 (49, 68)	67.5 (66, 77)	0.01	70.5 (69, 73)	0.11
Female	10 (77)	9 (64)	0.48	3 (38)	0.10
Body surface area (m <sup>2</sup> )	1.72 (1.58, 2.08)	2.1 (1.99, 2.27)	0.01	1.9 (1.6, 2.2)	0.94
Systolic blood pressure (mmHg)	123.38 ± 16.2	138.14 ± 17.6	0.03	130.75 ± 13.69	0.97
Diastolic blood pressure (mmHg)	68.46 ± 11.93	74.7 ± 12.4	0.20	72.38 ± 10.77	0.89
Heart rate (b.p.m.)	80.6 ± 15.5	73.6 ± 14.5	0.24	63.5 ± 9.1	0.02
Race			0.02		
White	6 (46)	5 (36)			
Black	0 (0)	6 (43)			
Unspecified	7 (54)	3 (21)			
Co-morbidities					
Coronary artery disease	2 (15)	7 (50)	0.06		
Systemic hypertension	6 (46)	12 (86)	0.03		
Hyperlipidaemia	2 (15)	11 (79)	0.001		
Diabetes mellitus	3 (23)	5 (36)	0.47		
Chronic kidney disease	4 (31)	6 (43)	0.52		
Atrial fibrillation	4 (31)	5 (36)	0.79		
Smoker	0 (0)	2 (14)	0.16		
COPD	3 (23)	6 (43)	0.28		
Obstructive sleep apnoea	2 (15)	10 (71)	0.003		
Medications					
ACE-inhibitor or ARB	4 (31)	8 (57)	0.17		
Beta-blocker	3 (23)	6 (43)	0.28		
Calcium channel blocker	5 (38)	3 (21)	0.33		
Nitrate	0 (0)	1 (7)	0.33		
Loop diuretic	5 (38)	12 (86)	0.01		
Thiazide diuretic	3 (23)	0 (0)	0.06		
Aldosterone blocker	5 (38)	9 (64)	0.18		
PDE5 inhibitor	6 (46)	1 (7)	0.02		
ERA	3 (23)	1 (7)	0.24		
Prostacyclin	2 (15)	0 (0)	0.13		
NYHA functional class			0.81		
Class I	1 (8)	1 (7)			
Class II	8 (62)	7 (50)			
Class III	4 (31)	6 (43)			
Class IV	0 (0)	0 (0)			
Laboratory data					
Creatinine (mg/dL)	0.9 (0.9, 1.2)	1.1 (1.0, 1.2)	0.50	0.95 (0.8, 1.2)	0.31
Haematocrit	0.38 (0.36, 0.42)	0.39 (0.36, 0.42)	0.50	0.41 (0.39, 0.42)	0.31

ACE, angiotensin-converting enzyme; ARB, angiotensin receptor blocker; COPD, chronic obstructive pulmonary disease; ERA, endothelin receptor antagonist; NYHA, New York Heart Association; PAH, pulmonary arterial hypertension; PDE5, phosphodiesterase type 5; PH-HFpEF, heart failure with preserved ejection fraction and pulmonary hypertension.

Categorical variables are presented as counts and percentages. Normally distributed continuous variables are presented as mean ± standard deviation. Non-normally distributed continuous variables are presented as median (25th percentile, 75th percentile).

\*P-value for PAH vs. PH-HFpEF.

†P-value for control vs. PH (combined PAH and PH-HFpEF cohorts).

we found that the ICC for RV native T1 was 0.87 and COV was 4.3%. The ICC for RV ECV was 0.94, and COV was 7.8%.

## Discussion

In this analysis, we comprehensively phenotyped patients with PH-HFpEF and PAH through CMR, echocardiography, and invasive haemodynamics and subsequently compared the extent and clinical correlates of diffuse RV fibrosis. To our knowledge, this is the first study to evaluate RV ECV in patients with both PH-HFpEF and PAH. Our study highlights the following points: (i) both PH-HFpEF and PAH patients have significantly higher degrees of diffuse RV fibrosis than

controls; (ii) diffuse RV fibrosis is present in these cohorts in the setting of relatively preserved RVEF; (iii) despite lower TPR in PH-HFpEF compared with PAH, the degree of diffuse RV fibrosis is similar in these groups; and (iv) in contrast to PAH, RV fibrosis in PH-HFpEF is strongly correlated to several indices of intrinsic RV myocardial remodelling but not RV afterload.

### Right ventricular dysfunction in heart failure with preserved function: a poor prognosis

In HFpEF, the onset of RV systolic dysfunction is strongly linked to adverse clinical outcomes. Indeed, several indices

**Table 2** Right heart catheterization haemodynamics, stratified by type of pulmonary hypertension

Parameter	PAH (n = 13)	PH-HFpEF (n = 14)	P-value
Right atrium (mmHg)	8 (6, 11)	11 (9, 15)	0.14
Right ventricular systolic pressure (mmHg)	77.2 ± 12.5	50.6 ± 13.5	0.01
Right ventricular diastolic pressure (mmHg)	6.6 ± 4.1	6.9 ± 3.7	0.34
Pulmonary artery systolic pressure (mmHg)	77.2 ± 13.4	50.6 ± 13.8	0.01
Pulmonary artery diastolic pressure (mmHg)	29 (23, 36)	21.5 (18, 25)	0.01
Mean pulmonary artery pressure (mmHg)	47.7 ± 8.4	33.8 ± 7.1	0.01
Transpulmonary gradient (mmHg)	33 (31, 39)	12.5 (10, 19)	0.01
Diastolic pulmonary gradient (mmHg)	14 (11, 23)	2.5 (0, 5)	0.01
Pulmonary capillary wedge pressure (mmHg)	10 (9, 15)	18 (15, 21)	0.01
Cardiac output (L/min)	5.29 (4.1, 5.9)	5.40 (4.7, 6.2)	0.33
Cardiac index (L/min/m <sup>2</sup> )	2.7 (2.3, 3.1)	2.49 (2.2, 2.9)	0.76
Pulmonary vascular resistance (WU)	6.34 (5.7, 10)	2.04 (1.9, 2.9)	0.01
Total pulmonary resistance (WU)	8.59 (8.1, 12.6)	5.68 (4.7, 7.7)	0.01

PAH, pulmonary arterial hypertension; PH-HFpEF, heart failure with preserved ejection fraction and pulmonary hypertension. Normally distributed continuous variables are presented as mean ± standard deviation. Non-normally distributed continuous variables are presented as median (25th percentile, 75th percentile).

**Table 3** Cardiovascular magnetic resonance characteristics, stratified by type of pulmonary hypertension

Parameter	PAH (n = 13)	PH-HFpEF (n = 13)	P-value*	Control (n = 8)	P-value <sup>†</sup>
LV end-diastolic volume index (mL/m <sup>2</sup> )	74.5 ± 10.1	73.7 ± 25.1	0.67	79.8 ± 11.3	0.62
LV end-systolic volume index (mL/m <sup>2</sup> )	30.1 ± 6	31.4 ± 16.4	0.38	34.4 ± 5.6	0.68
LV stroke volume index (mL/m <sup>2</sup> )	44.3 ± 6.7	42.5 ± 11.6	0.77	45.4 ± 7.4	0.68
LV ejection fraction (%)	59.6 ± 5.7	56.5 ± 8.9	0.42	56.9 ± 4.0	0.28
LV mass index (g/m <sup>2</sup> )	40.8 ± 7.9	41.1 ± 9.7	0.39	42.9 ± 10.8	0.88
RV end-diastolic volume index (mL/m <sup>2</sup> )	102.9 (83.3, 122.9)	70.50 (54.7, 116.0)	0.11	83.17 (76.8, 91.1)	0.62
RV end-systolic volume index (mL/m <sup>2</sup> )	56.7 (39.0, 81.0)	42.01 (31.5, 70.2)	0.28	38.79 (36.9, 44.6)	0.20
RV stroke volume index (mL/m <sup>2</sup> )	43.6 ± 6.5	38.6 ± 13.1	0.1	44.7 ± 7.5	0.25
RV ejection fraction (%)	43.8 ± 11.1	42.3 ± 8.3	0.91	52.7 ± 4.2	0.01
Late gadolinium enhancement	12 (92)	5 (36)	0.002	4 (50)	0.51
RV native T1 (ms)	1126 ± 101.1	1136 ± 109.5	0.88	1012 ± 106.0	0.01
LV lateral native T1 (ms)	1062 ± 73.3	1035 ± 56.7	0.29	1023 ± 43.8	0.31
RV ECV (%)	34.0 ± 4.5	33.1 ± 8.0	0.57	26.4 ± 4.2	0.01
LV lateral ECV (%)	30.3 ± 6.0	26.2 ± 5.3	0.06	25.2 ± 3.2	0.25
RV global longitudinal strain (%)	-13.6 ± 3.0	-15.0 ± 3.5	0.34	-16.1 ± 1.8	0.17
RV free wall longitudinal strain (%)	-15.2 ± 4.5	-17.2 ± 3.9	0.29	-18.1 ± 3.2	0.28
RV global early diastolic strain (%)	105.5 ± 37.2	114.0 ± 44.7	0.99	107.9 ± 21.9	0.65
RV free wall early diastolic strain (%)	129.2 ± 36.6	132.0 ± 32.1	0.88	119.1 ± 33.2	0.32

ECV, extracellular volume; LA, left atrial; LV, left ventricular; PAH, pulmonary arterial hypertension; PH-HFpEF, heart failure with preserved ejection fraction and pulmonary hypertension; RV, right ventricular.

Categorical variables are presented as counts and percentages. Normally distributed continuous variables are presented as mean ± standard deviation. Non-normally distributed continuous variables are presented as median (25th percentile, 75th percentile).

\*P-value for PAH vs. PH-HFpEF.

<sup>†</sup>P-value for control vs. PH.

of RV systolic dysfunction, including both reduced fractional area change and RVEF < 45%, have been associated with all-cause mortality in HFpEF independent of degree of PH.<sup>3,4</sup> Given the grim clinical implications of RV dysfunction in HFpEF, there is an unmet need to not only to understand the mechanistic basis of this syndrome but also to identify the presence of RV pathology prior to the onset of overt systolic derangement. Quantification of diffuse RV fibrosis by CMR thus offers promise in elucidating mechanisms of RV dysfunction and identifying HFpEF patients with subclinical adverse remodelling who may benefit from future targeted therapies to prevent further progression.

### Measurement of right ventricular fibrosis with cardiovascular magnetic resonance

Cardiovascular magnetic resonance is the most frequently used non-invasive imaging modality for assessing both focal and diffuse myocardial fibrosis by measuring the longitudinal relaxation time (T1) of myocardial tissue. Determination of ECV by T1 estimation using the MOLLI sequence enables quantitation of diffuse LV fibrosis in a variety of cardiomyopathies, including HFpEF.<sup>11–14</sup> Unlike LV fibrosis, measurement of diffuse RV fibrosis is challenging on account of the chamber's thin-walled myocardium. Because of these challenges, relatively few studies have evaluated RV fibrosis

**Figure 2** Comparison of box-and-whisker plots and mean values of (A) right ventricular (RV) native T1 and (B) RV extracellular volume (RV ECV) in controls, pulmonary arterial hypertension (PAH), and pulmonary hypertension and heart failure with preserved ejection fraction (PH-HFpEF). PH, pulmonary hypertension.

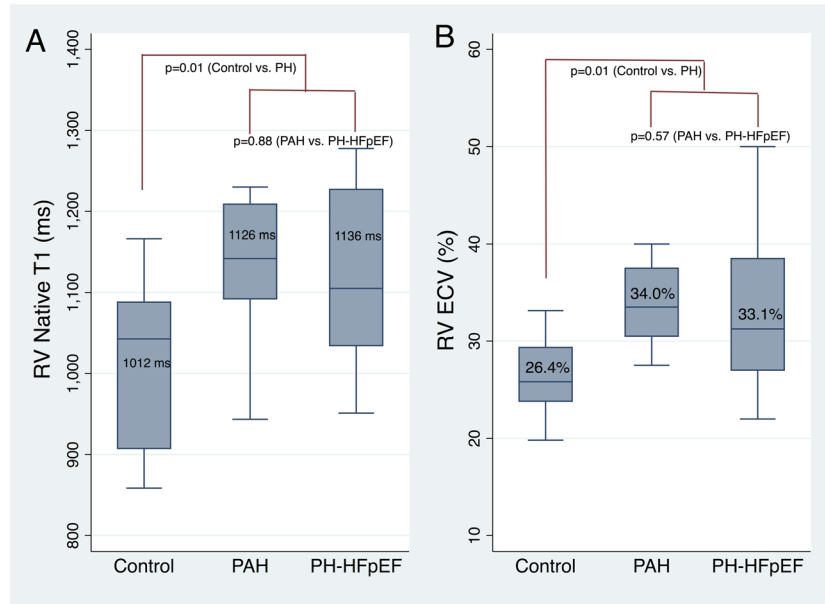
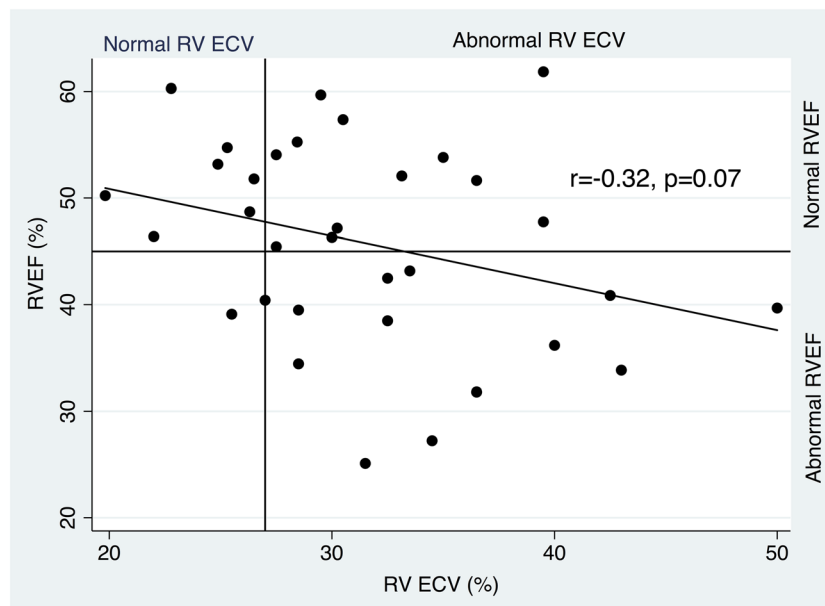


**Figure 3** Relationship between right ventricular extracellular volume (RV ECV) and RV ejection fraction (RVEF) highlighting the subjects with elevated RV ECV but normal RVEF. Vertical line represents cut-off (27%) between normal and abnormal RV ECV. Horizontal line represents cut-off (45%) between normal and abnormal RVEF. Diagonal line represents linear fit of the relationship between RV ECV and RVEF.



using CMR-derived T1 mapping in other cardiovascular disease states, including non-ischaemic cardiomyopathy and PAH.<sup>15–17</sup> To overcome inherent limitations with conventional CMR techniques for RV fibrosis assessment, we

optimized a high-resolution MOLLI sequence and utilized this high-resolution sequencing to compare the degree and correlates of RV fibrosis in two populations at elevated risk for RV dysfunction (PH-HFpEF and PAH).

**Table 4** Correlations between RV ECV and echocardiographic, CMR, and invasive haemodynamic parameters in PAH and PH-HFpEF subjects

	PAH		PH-HFpEF	
	<i>r</i>	<i>P</i> -value	<i>r</i>	<i>P</i> -value
<b>Echocardiographic parameters</b>				
LV ejection fraction	-0.27	0.42	-0.67	0.01
LV end-diastolic volume index	0.32	0.34	0.61	0.03
LV end-systolic volume index	0.46	0.16	0.62	0.03
LA volume index	0.10	0.62	0.89	<0.001
Early transmitral (E) velocity	0.12	0.56	0.73	0.003
Late transmitral (A) velocity	-0.72	0.01	-0.53	0.15
E/A ratio	0.83	0.002	0.65	0.04
e' velocity (lateral)	-0.33	0.33	-0.63	0.03
RV diastolic stiffness	0.52	0.11	0.70	0.01
<b>CMR parameters</b>				
LV end-diastolic volume index	0.16	0.59	0.83	<0.001
LV end-systolic volume index	0.03	0.93	0.83	<0.001
LV stroke volume index	0.27	0.37	0.62	0.02
RV end-diastolic volume index	0.05	0.87	0.67	0.01
RV end-systolic volume index	0.04	0.90	0.62	0.02
RV stroke volume index	0.30	0.34	0.62	0.02
RV ejection fraction	-0.12	0.71	-0.35	0.24
RV global longitudinal strain	0.21	0.48	0.57	0.04
RV free wall longitudinal strain	0.24	0.43	0.59	0.03
<b>RHC parameters</b>				
Pulmonary vascular resistance	0.63	0.02	0.20	0.49
Total pulmonary resistance	0.57	0.04	0.08	0.79

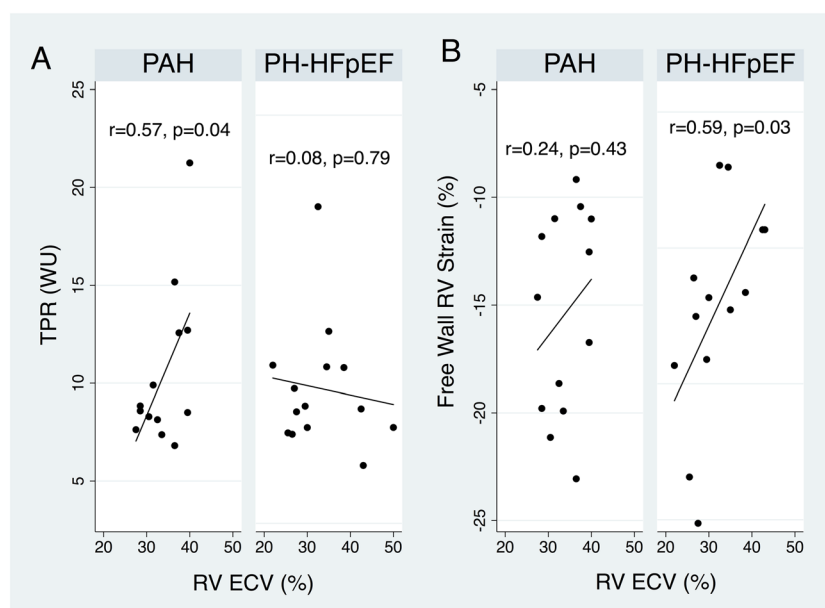
CMR, cardiac magnetic resonance; ECV, extracellular volume; LA, left atrial; LV, left ventricular; PAH, pulmonary arterial hypertension; PH-HFpEF, heart failure with preserved ejection fraction and pulmonary hypertension; RHC, right heart catheterization; RV, right ventricular.

## Right ventricular fibrosis in pulmonary arterial hypertension and pulmonary hypertension and heart failure with preserved ejection fraction

Right ventricular dysfunction in HFpEF may be a downstream consequence of PH because of elevated LV filling pressures (i.e. load-dependent mechanism) or intrinsic RV pathology (i.e. load-independent mechanisms), but the extent to which either of these processes is contributing is not known.<sup>3,4,18,19</sup> Indeed, several clinical factors have been implicated in driving RV dysfunction through load-independent phenomena, including atrial fibrillation, diastolic ventricular interdependence, coronary artery disease, and renal dysfunction.<sup>19</sup>

In our study, RV fibrosis and dysfunction were similar in both PH-HFpEF and PAH despite significantly lower RV afterload in the PH-HFpEF group. Unlike PAH, in which RV ECV was strongly associated with TPR, RV ECV in PH-HFpEF was significantly associated with measures of myocardial remodelling including LV, LA, and RV chamber enlargement, higher RV myocardial stiffness, and reduced RV strain. In aggregate, our findings suggest that intrinsic myocardial changes may play an integral role in the evolution of RV dysfunction and may be more influential than haemodynamic alterations in the PH-HFpEF cohort. It is also possible that patients with PH-HFpEF are uniquely sensitive to moderate elevations in RV afterload, which further suggests underlying, intrinsic RV myocardial pathology in PH-HFpEF compared with PAH.

**Figure 4** Relationship between (A) RV ECV with (A) total pulmonary resistance (TPR) and (B) right ventricular (RV) free wall strain in pulmonary arterial hypertension (PAH) and pulmonary hypertension and heart failure with preserved ejection fraction (PH-HFpEF) subjects. Lines represent linear fit of the relationship between RV extracellular volume (RV ECV) and TPR or RV free wall strain.



Previous studies have demonstrated increased RV myocardial stiffness in both PAH and HFpEF patients.<sup>3,20</sup> Increased collagen and stiffening of RV cardiomyocyte sarcomeres have been noted in patients with PAH.<sup>20</sup> Interestingly, increased RV stiffness in this group was associated with increased RV contractility, suggesting a compensatory mechanism in the setting of increased RV afterload. In contrast, in HFpEF, there appears to be a reduction in the RV adaptive response to increased RV afterload.<sup>3</sup> This finding may account for the similar degree of RV fibrosis and dysfunction across all case subjects in our study despite the relatively lower TPR in the PH-HFpEF group.

While pulmonary vasodilators are a mainstay of therapy in PAH, there is limited evidence for their use in PH-HFpEF. In murine models of PAH, certain pulmonary vasodilators may reduce RV fibrosis, likely due to favourable effects on RV afterload.<sup>21,22</sup> Further investigations are required to determine if these therapies result in reduction in RV fibrosis in humans with PAH or PH-HFpEF.

### Right ventricular diffuse fibrosis: early identification of right ventricular pathology

In contrast to other populations,<sup>23</sup> we did not find a significant correlation between RV ECV and RVEF in PH-HFpEF or PAH cohorts. The lack of association between subclinical anatomic change (i.e. diffuse fibrosis) and overt functional remodelling in our study suggests that RV ECV is not a surrogate of RVEF and should be viewed as a unique marker of RV remodelling. Additionally, our findings suggest that RV fibrosis may precede RV systolic dysfunction and thus may serve as a marker for early identification RV pathology in PH-HFpEF.

### Limitations

Our study has several potential limitations. While the sample size of this study is adequate to assess the feasibility of this RV T1 mapping technique in humans as well as to evaluate associations between RV ECV and other subject parameters, the small number of subjects may have led to type I errors; therefore, nominally significant *P*-values should be interpreted with caution. However, this study represents a unique population of both PH-HFpEF and PAH that was comprehensively characterized through high-resolution CMR, echocardiography, and invasive haemodynamics to allow for insights into pathophysiological differences between these two syndromes. Associations in single-centre observational data do not establish causality and could represent unmeasured confounders perhaps related to referral biases. Although our slice positioning and breath-holding techniques mitigated partial volume effects, RV T1 mapping

on parametric maps particularly in controls remains challenging owing to the thin RV wall, adjacent epicardial fat, and fat/water artefacts. While the correlation between diffuse RV fibrosis as detected by HR-MOLLI sequence and histological RV fibrosis is not known, the similarity of RV ECV values in our PAH population compared with other PAH cohorts suggests that HR-MOLLI is accurate in determining RV fibrosis in humans. Because of the collection of invasive haemodynamic measurements in case subjects, natriuretic peptides were not obtained as part of the study protocol. As control subjects did not undergo echocardiography, we were unable to compare echocardiographic indices of RV function between case subjects and controls. Finally, there is a need for more normative data to better understand the significance of a particular RV ECV value in a patient with known or suspected RV pathology.

## Conclusions

In this analysis of a comprehensively phenotyped cohort of patients with PH, PH-HFpEF patients had a similar extent of diffuse RV fibrosis despite significantly lower RV afterload compared with PAH patients. While diffuse RV fibrosis as measured by RV ECV was correlated with degree of pulmonary vasculopathy in PAH, there was no significant correlation between RV ECV and RV afterload among the PH-HFpEF cohort. Diffuse RV fibrosis is strongly associated with worse indices of LV and RV myocardial structure and function in PH-HFpEF, suggesting that load-independent mechanisms may be driving RV remodelling and subsequent dysfunction in this cohort. RV ECV was not correlated with RVEF, suggesting that diffuse RV fibrosis may precede functional remodelling and could identify a high-risk cohort who may benefit from targeted therapies to prevent progression of RV dysfunction.

## Acknowledgements

The authors would like to thank Marisol Bello, Rebecca Ditch, and Rachel Davids for their assistance with scanning and blood draws as well as Caitlin Brady for her assistance in recruitment and scheduling. We are indebted to Bruce Spottiswoode, PhD, for his assistance in optimizing the HR-MOLLI sequence and Michael Cuttica, MD, for his help in recruiting subjects with PAH.

## Conflict of interest

S.J.S. was supported by the National Institutes of Health Grants R01 HL105755, R01 HL127028, and R01 HL140731

and American Heart Association Grants 16SFRN28780016 and 15CVGSPD27260148 and has received research grants from Actelion, AstraZeneca, Corvia, and Novartis and consulting fees from Actelion, Amgen, AstraZeneca, Bayer, Boehringer-Ingelheim, Cardiara, Eisai, Ironwood, Merck, Novartis, Sanofi, Tenax, and United Therapeutics. All the remaining authors have nothing to disclose.

## Funding

R.B.P. is supported by the National Heart, Lung, and Blood Institute T32 postdoctoral training grant (T32HL069771). B. H.F. is supported by Northwestern University Eleanor Wood-Prince Grant Initiative, Chicago, Illinois, and International Society for Heart & Lung Transplantation/Bayer Pulmonary Hypertension Research Award, Addison, Texas.

## References

- Mohammed SF, Hussain I, AbouEzzedine OF, Takahama H, Kwon SH, Forfia P, Roger VL, Redfield MM. Right ventricular function in heart failure with preserved ejection fraction: a community-based study. *Circulation* 2014; 23; **130**: 2310–2320.
- Burke MA, Katz DH, Beussink L, Selvaraj S, Gupta DK, Fox J, Chakrabarti S, Sauer AJ, Rich JD, Freed BH, Shah SJ. Prognostic importance of pathophysiologic markers in patients with heart failure and preserved ejection fraction. *Circ Heart Fail* 2014; 7: 288–299.
- Melenovsky V, Hwang SJ, Lin G, Redfield MM, Borlaug BA. Right heart dysfunction in heart failure with preserved ejection fraction. *Eur Heart J* 2014; **35**: 3452–3462.
- Aschauer S, Kammerlander AA, Zotter-Tufaro C, Ristl R, Pfaffenberger S, Bachmann A, Duca F, Marzluf BA, Bonderman D, Mascherbauer J. The right heart in heart failure with preserved ejection fraction: insights from cardiac magnetic resonance imaging and invasive haemodynamics. *Eur J Heart Fail* 2016; **18**: 71–80.
- Zakeri R, Mohammed SF. Epidemiology of right ventricular dysfunction in heart failure with preserved ejection fraction. *Curr Heart Fail Rep* 2015; **12**: 295–301.
- Gorter TM, Hoendermis ES, van Veldhuisen DJ, Voors AA, Lam CS, Geelhoed B, Willems TP, van Melle JP. Right ventricular dysfunction in heart failure with preserved ejection fraction: a systematic review and meta-analysis. *Eur J Heart Fail* 2016; **18**: 1472–1487.
- Lam CS, Roger VL, Rodeheffer RJ, Borlaug BA, Enders FT, Redfield MM. Pulmonary hypertension in heart failure with preserved ejection fraction: a community-based study. *J Am Coll Cardiol* 2009; **53**: 1119–1126.
- McKee PA, Castelli WP, McNamara PM, Kannel WB. The natural history of congestive heart failure: the Framingham study. *N Engl J Med* 1971; **285**: 1441–1446.
- Kellman P, Wilson JR, Xue H, Ugander M, Arai AE. Extracellular volume fraction mapping in the myocardium, part 1: evaluation of an automated method. *Journal of Cardiovascular Magnetic Resonance: Official Journal of the Society for Cardiovascular Magnetic Resonance* 2012; **14**: 63.
- Moon JC, Messroghli DR, Kellman P, Piechnik SK, Robson MD, Ugander M, Gatehouse PD, Arai AE, Friedrich MG, Neubauer S, Schulz-Menger J, Schelbert EB, Society for Cardiovascular Magnetic Resonance I, Cardiovascular Magnetic Resonance Working Group of the European Society of C. Myocardial T1 mapping and extracellular volume quantification: a Society for Cardiovascular Magnetic Resonance (SCMR) and CMR Working Group of the European Society of Cardiology consensus statement. *J Cardiovasc Magn Reson* 2013; **14**: 92.
- Rommel KP, von Roeder M, Latuscynski K, Oberueck C, Blazek S, Fengler K, Besler C, Sandri M, Lucke C, Gutberlet M, Linke A, Schuler G, Lurz P. Extracellular volume fraction for characterization of patients with heart failure and preserved ejection fraction. *J Am Coll Cardiol* 2016; **67**: 1815–1825.
- Messroghli DR, Radjenovic A, Kozierke S, Higgins DM, Sivanathan MU, Ridgway JP. Modified look-locker inversion recovery (MOLLI) for high-resolution T1 mapping of the heart. *Magn Reson Med* 2004; **52**: 141–146.
- Flett AS, Hayward MP, Ashworth MT, Hansen MS, Taylor AM, Elliott PM, McGregor C, Moon JC. Equilibrium contrast cardiovascular magnetic resonance for the measurement of diffuse myocardial fibrosis: preliminary validation in humans. *Circulation* 2010; **122**: 138–144.
- Mongeon FP, Jerosch-Herold M, Coelho-Filho OR, Blankstein R, Falk RH, Kwong RY. Quantification of extracellular matrix expansion by CMR in infiltrative heart disease. *JACC Cardiovasc Imaging* 2012; **5**: 897–907.
- Jellis CL, Yingchoncharoen T, Gai N, Kusunose K, Popovic ZB, Flamm S, Kwon D. Correlation between right ventricular T1 mapping and right ventricular dysfunction in non-ischemic cardiomyopathy. *Int J Cardiovasc Imaging* 2018; **34**: 55–65.
- Kawel-Boehm N, Dellas Buser T, Greiser A, Bieri O, Bremerich J, Santini F. In-vivo assessment of normal T1 values of the right-ventricular myocardium by cardiac MRI. *Int J Cardiovasc Imaging* 2014; **30**: 323–328.
- Mehta BB, Chen X, Bilchick KC, Salerno M, Epstein FH. Accelerated and navigator-gated look-locker imaging for cardiac T1 estimation (ANGIE): development and application to T1 mapping of the right ventricle. *Magn Reson Med* 2015; **73**: 150–160.
- Tedford RJ, Hassoun PM, Mathai SC, Giris RE, Russell SD, Thieman DR, Cingolani OH, Mudd JO, Borlaug BA, Redfield MM, Lederer DJ, Kass DA. Pulmonary capillary wedge pressure

## Supporting information

Additional supporting information may be found online in the Supporting Information section at the end of the article.

**Supplemental Table S1:** Echocardiographic Characteristics, Stratified by Type of Pulmonary Hypertension

**Supplemental Table S2:** Association of RV ECV in all PH Subjects with Echocardiographic, CMR, and Invasive Hemodynamic Parameters

**Supplemental Table S3:** Association of LV ECV in all PH subjects with Echocardiographic, CMR, and Invasive Hemodynamic Parameters

**Supplemental Table S4:** Association of LV ECV in PAH and PH-HFpEF subjects with Echocardiographic, CMR, and Invasive Hemodynamic Parameters

- augments right ventricular pulsatile loading. *Circulation* 2012; **125**: 289–297.
19. Gorter TM, van Veldhuisen DJ, Bauersachs J, Borlaug BA, Celutkiene J, Coats AJS, Crespo-Leiro MG, Guazzi M, Harjola VP, Heymans S, Hill L, Lainscak M, Lam CSP, Lund LH, Lyon AR, Mebazaa A, Mueller C, Paulus WJ, Pieske B, Piepoli MF, Ruschitzka F, Rutten FH, Seferovic PM, Solomon SD, Shah SJ, Triposkiadis F, Wachter R, Tschope C, de Boer RA. Right heart dysfunction and failure in heart failure with preserved ejection fraction: mechanisms and management. Position statement on behalf of the Heart Failure Association of the European Society of Cardiology. *Eur J Heart Fail* 2018; **20**: 16–37.
  20. Rain S, Handoko ML, Trip P, Gan CT, Westerhof N, Stienen GJ, Paulus WJ, Ottenheijm CA, Marcus JT, Dorfmueller P, Guignabert C, Humbert M, Macdonald P, Dos Remedios C, Postmus PE, Saripalli C, Hidalgo CG, Granzier HL, Vonk-Noordegraaf A, van der Velden J, de Man FS. Right ventricular diastolic impairment in patients with pulmonary arterial hypertension. *Circulation* 2013; **128**: 2016–2025 2011-2010.
  21. Schafer S, Ellinghaus P, Janssen W, Kramer F, Lustig K, Milting H, Kast R, Klein M. Chronic inhibition of phosphodiesterase 5 does not prevent pressure-overload-induced right-ventricular remodelling. *Cardiovasc Res* 2009; **82**: 30–39.
  22. Borgdorff MA, Bartelds B, Dickinson MG, van Wiechen MP, Steendijk P, de Vroomen M, Berger RM. Sildenafil treatment in established right ventricular dysfunction improves diastolic function and attenuates interstitial fibrosis independent from afterload. *Am J Physiol Heart Circ Physiol* 2014; **307**: H361–H369.
  23. Mehta BB, Auger DA, Gonzalez JA, Workman V, Chen X, Chow K, Stump CJ, Mazimba S, Kennedy JL, Gay E, Salerno M, Kramer CM, Epstein FH, Bilchick KC. Detection of elevated right ventricular extracellular volume in pulmonary hypertension using Accelerated and Navigator-Gated Look-Locker Imaging for Cardiac T1 Estimation (ANGIE) cardiovascular magnetic resonance. *J Cardiovasc Magn Reson* 2015; **17**: 110.